Arch. Metall. Mater. **66** (2021), 2, 469-476

DOI: 10.24425/amm.2021.135880

D. VARANASI[1], K.E. ALDAWOUDI[1,2], P. BAUMLI[1], D. KONCZ-HORVATH[1], G. KAPTAY[1,3*]

NON-WETTING TO WETTING TRANSITION TEMPERATURES OF LIQUID TIN ON SURFACES OF DIFFERENT STEEL SAMPLES CORRESPONDING TO THEIR SPONTANEOUS DEOXIDATION

The goal of this paper is to measure the non-wetting to wetting transition temperatures of liquid tin on surfaces of different steel samples in vacuum with residual pressure of 10^{-8} bar. The experiments were conducted on four steels (C45, S103, CK60 and EN1.4034) of varying compositions using pure tin (99.99%) by the sessile drop method. Non-wetting to wetting transition (contact angle decreasing below 90°) by liquid tin was observed as function of increasing temperature in the range of 820-940 K for low alloyed steels C45, S103 and CK60, while it was considerably higher (around 1130 K) for high chromium EN1.4034 steel. It is concluded that at about the same temperatures, the surfaces of the steel samples are spontaneously deoxidized due to the combined effect of high temperature, low vacuum and C-content of steels. After the oxide layer is removed, the contact angles of liquid tin on steel surfaces were found in the range of 45-80° for low alloyed C45, S103 and CK60 steels and around 20° for high chromium EN1.4034 steel. These relatively high contact angle values compared to other metal/metal couples (such as liquid Cu on steels) are due to the formation of not fully metallic intermetallic compounds (FeSn and $FeSn_2$) at the interface (such do not form in the Cu/Fe system).

Keywords: wetting transition, deoxidation, contact angles, steels, liquid tin

1. Introduction

Wetting as a sub-field of interface science has garnered attention since the early 19th century [1]. Industrialization leading to the need for advancement in structural fabrication has revolutionized the metallurgical joining techniques in which wetting plays a major role. Definition of wetting, its importance and various factors affecting the wetting were discussed in detail in [1-10] (see also Fig. 1):

$$\cos\theta = \frac{\sigma_{sv} - \sigma_{sl}}{\sigma_{lv}} = \frac{W_a}{\sigma_{lv}} - 1 \qquad (1)$$

where, θ (°) is the contact angle of a liquid on a surface of solid, σ_{sv} (J/m^2) is the surface energy of the solid, σ_{sl} (J/m^2) is the solid-liquid interfacial energy, σ_{lv} is the surface tension of the liquid, W_a (J/m^2) is the adhesion energy between solid and liquid.

The equilibrium contact angle depends on the nature of the contacting liquid and solid phases [11-13]. Depending on the nature of the solid/liquid couples in the given experiment, three types of wetting are defined: non-reactive wetting [11], reactive wetting [11] and dissolutive wetting [12-13]. Usual wetting

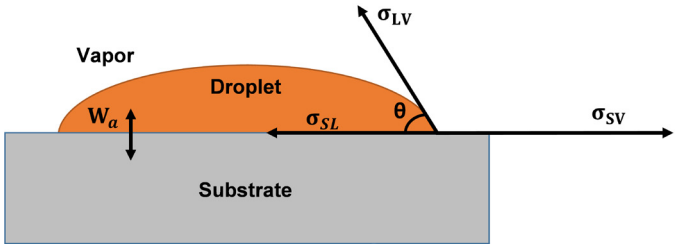

Fig. 1. Schematic of wetting of a liquid droplet on a solid surface

studies were carried out using sessile drop technique. Depending on method of formation of sessile drop, the technique was classified into two modes: the classical contact heating method and the dispensed drop method [14]. Some methodological issues, advancements and improvements in the experimentation techniques were discussed in [15-17].

Steels are usually covered with a native oxide layer at room temperature under normal conditions. The common oxide is Fe_2O_3 [18-19], but it varies as function of composition of the steel with Cr_2O_3 dominating the high Cr-steels [20]. Evolution of oxide layers on various steel surfaces and their subsequent

[1] UNIVERSITY OF MISKOLC, INSTITUTE OF PHYSICAL METALLURGY, METAL FORMING AND NANOTECHNOLOGY, 3515 MISKOLC-EGYETEMVAROS, HUNGARY
[2] UNIVERSITY OF BABYLON, COLLEGE OF MATERIALS ENGINEERING, IRAQ
[3] MTA-ME MATERIALS SCIENCE RESEARCH GROUP, 3515 MISKOLC-EGYETEMVAROS, HUNGARY

* Corresponding author: kaptay@hotmail.com

deoxidation was discussed in the literature [21-26]. The steel surface deoxidation is due to the chemical interaction of carbon dissolved in steel with the oxide covering its surface leading to the formation of volatile CO / CO_2 [19,22,25]. Furthermore, non-wetting to wetting transition temperature of liquid Cu-Ag alloy due to deoxidation of the originally oxidized surface of a stainless steel was found by Kozlova et al. [22].

Metal/metal wetting systems were in focus of scientific investigations mostly for joining materials. Since Sn-alloys and Cu-alloys are mostly used as joining materials in form of solders and brazes, the research is highly focused on them. A brief review of the vast literature available in metal/metal wetting systems is presented here. Wetting of metallic liquids like Cu, Sn, Ag and Au on their own solid surfaces was reported in [2,27] and contact angles in the range of 0-10° were reported by them. The contact angles of liquid Sn on surface of pure iron were reported in the range of 30-60° in the temperature range between 673-1000 K [28-29]. Wetting between different metallic solid/liquid systems was also studied in the literature [30-32]. Liquid Sn and Sn based alloys were used for wetting characteristics on various metallic substrates and the formation of various Sn-intermetallic compounds were reported in [33-37]. Similar results were published by [38] with Cu and Ni as solid substrates and when Sn-alloys (In, Zn, Cu) were used as molten liquids. The wettability of tin based alloy solders on the laser treated steel surfaces were reported in [39-42]. Wetting by Sn and Sn-Zn alloys of varying compositions on Cu and Al substrates were discussed by [43] under inert gas environment between 250-500°C. They concluded liquid Sn-Zn alloys need protective environment for good wetting of metallic substrates [44]. More recently, similar experimental results were also reported in [45-46] where the focus was kept on formation of intermetallic layers during the wetting by Sn-alloys.

In the present paper, tin is selected as an appropriate metal to study non-wetting -to- wetting transitions on steel substrates starting from a relatively low temperature to a relatively high temperature. The transition temperature to be measured is attributed to the spontaneous removal of the oxide layer from steel surface, as already proven in the literature. However, the experimental findings reported in the literature so far are extended in this paper to other steel types.

2. Selection of a wetting/non-wetting metal

For our purposes, a metal is needed that satisfies the following requirements: (i) has a wide temperature range of its stability in liquid state, (ii) wets unoxidized steels with the contact angle below 90º, (iii) poorly wets oxidized steels with the contact angle above 90º. The latter condition is satisfied for the majority of liquid metals. Our final choice is tin. It has a relatively low melting point (505 K) and it is stable as a liquid up to 1,155 K at the residual pressure of 10^{-8} bar in vacuum (Fig. 2). Moreover, it is widely used as a basic component for soldering [47-48]. So, all the experiments were conducted in this study with liquid tin.

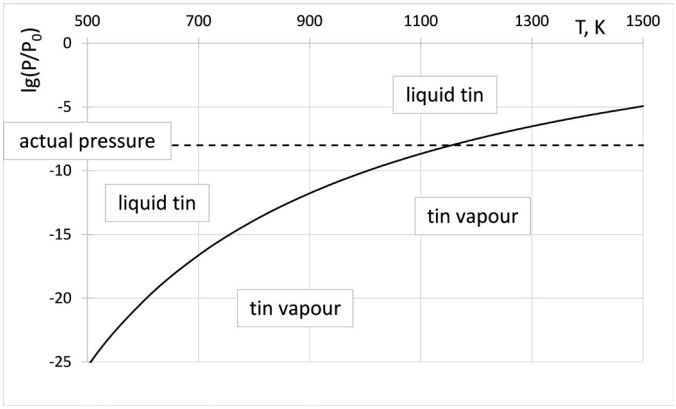

Fig. 2. Equilibrium vapor pressure of tin plotted as function of temperature calculated from data of [49]. The actual residual pressure in our furnace is shown by a horizontal dotted line; under these conditions tin is a stable liquid below 1155 K

3. Materials and Experimental

The compositions of the steels studied in this paper are tabulated in Table 1. The steel samples were cut to dimensions 10 mm × 7 mm × 4 mm. Then, the samples were ground with 180 µm, 220 µm and 320 µm grit size sandpapers before polishing with a 3 µm grit polishing paper using alumina paste for obtaining a mirror like finish. Pure Sn (99.99%) sample with mass in the range of 0.02-0.05 g was used for wetting experiments.

TABLE 1

Chemical composition of steels used in this study (mass %)

Steel	C	Cr	Mn	S	Fe
C45	0.45	—	0-0.5	0.030	Rest
S103	0.61	—	0.25	0.020	Rest
CK60	0.25	0.15	0.75	0.070	Rest
EN 1.4034	0.15	12	1.0	0.035	Rest

A solid tin piece was placed on the surface of steel (Fig. 3a) inside a resistance heating high vacuum furnace at a residual pressure of 10^{-8} bar. The furnace was equipped with Pt/Pt-Rh thermocouple for measuring the temperature with a heating rate of about 20°C/min. The experiments were conducted up to temperature of 1230 K. As the furnace is heated continuously,

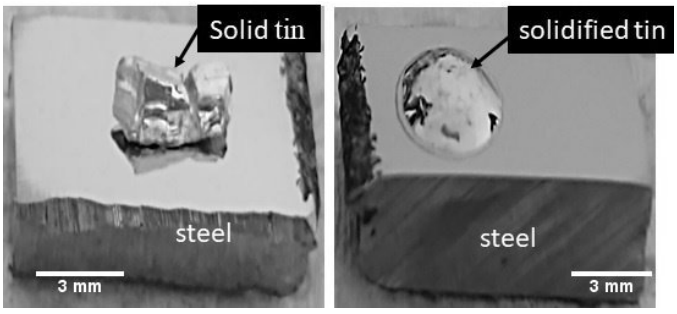

Fig. 3. Contact heating sessile drop arrangement of the wetting experiment. The solid tin piece before melting (Fig. 3a) and post experiment after cooling and solidification (Fig. 3b)

the solid tin melts and forms a molten droplet on the surface of steel. When tin is melted, it first forms a poorly wetting droplet on the oxidized surface of steel. Then, the system is being continuously heated further and at a special temperature the droplet spreads relatively fast, within 10 K, or so. The tin droplet during the experiments was continuously recorded by a video camera connected to the furnace via a computer making the image analysis possible for calculating contact angles. The contact angles were measured by using KSV software. The samples were then cooled down to room temperature via spontaneous cooling (left overnight), taken out and mounted in resin and polished for scanning electron microscopy (SEM) investigation using Carl Zeiss EVO MA10 equipment at 20 KV accelerating voltage.

In addition to energy dispersive X-ray spectroscopy (SEM-EDS), electron backscatter diffraction (SEM-EBSD) technique was used to identify different phases of the intermetallic compounds formed at the Fe/Sn interface. The SEM-EBSD was carried out using Thermoscientific Helios G4 PFIB CXe (EDAX HIKARI) equipment at 20 KV accelerating voltage.

4. Results and Discussion

As the Sn/steel couple is contact heated, tin melts at 505 K and forms a near spherical non-wetting shape on the surface of all steel samples. This is obviously due to the presence of oxide layer on surface of the steel samples [2,50]. However, as the temperature is increased, the near spherical non-wetting droplet of tin is gradually transformed into a wetting sessile droplet (Fig. 4).

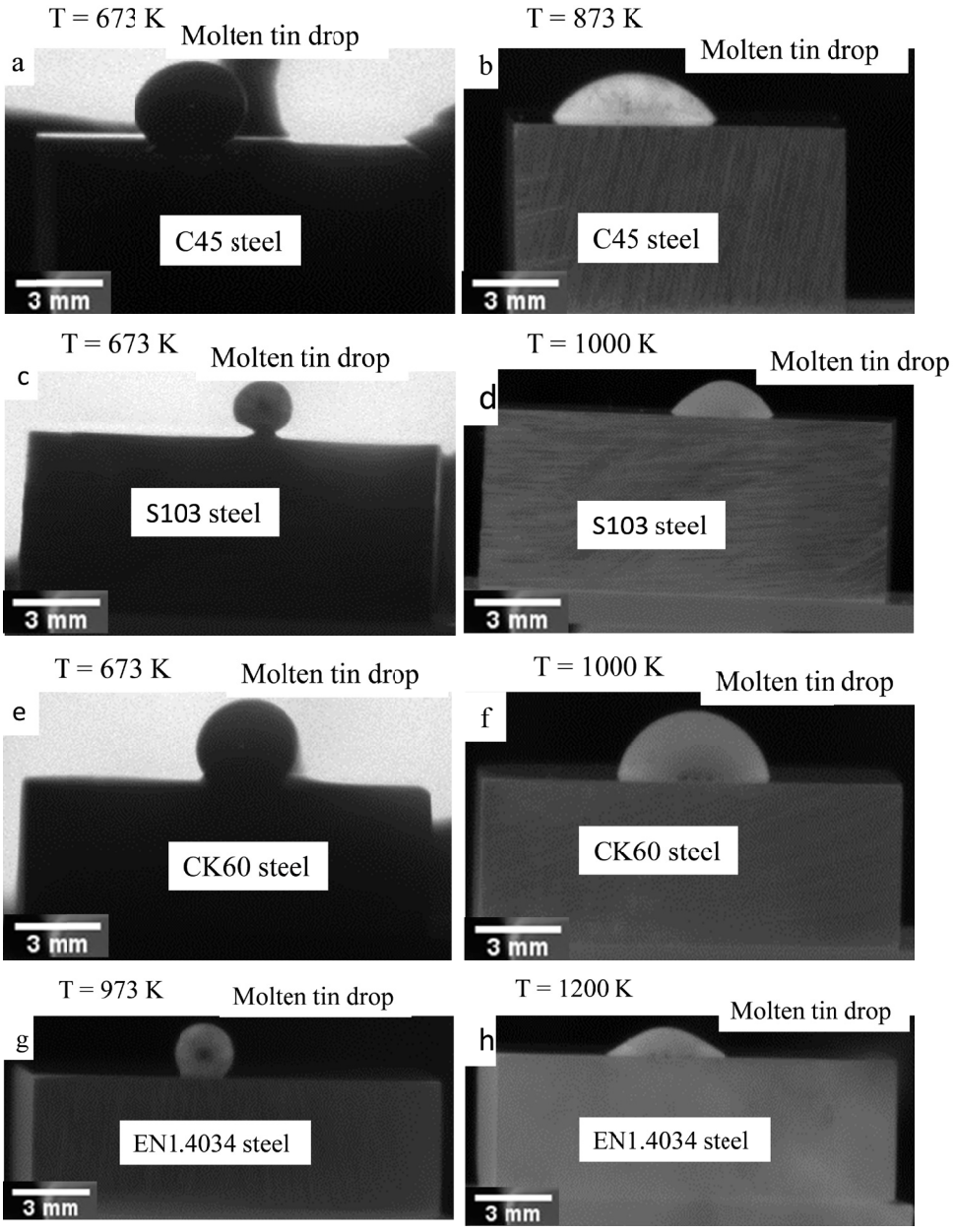

Fig. 4. Photographs of liquid tin droplets on various steel substrates at different temperatures. Figs. a, c, e and g show the non-wetting droplets, while Figs. b, d, f and h show the same tin droplets after the wetting transition. The unusual shape of a sessile drop in Fig. h is due to the formation and floating of $FeSn_x$ intermetallics to the upper drop surfac

The measured contact angles of liquid tin on different steels were plotted as function of temperature in Fig. 5. The transition temperatures measured from Fig. 5 are collected in Table 2 (similar transition temperature by liquid Cu-Ag eutectic was reported by Kozlova et al. [22] under similar conditions). Non-reactive liquid metals have weak adhesion energy with inert oxides due to weak van-der-Waals forces. When the oxide layer is removed and true metal/metal contact is established, the adhesion energy increases, and the contact angle decreases as follows from Eq. (1). In Table 2, the contact angles of liquid tin are also shown measured at temperatures exceeding the transition temperatures by 100 K. These measured contact angles values agree well with literature data [28-29].

Fig. 6 show post experimental cross-sectioned images of the interface formed between tin and various steels with formation of Fe-Sn intermetallic layer / particles at the interface. Intermetallic layer observed at the steel/Sn interface, a part of which is lifted up in the molten tin due to buoyancy force. The average thickness of intermetallic layer was found to be around 20 μm. EBSD analysis of the interface was also carried out to identify these intermetallic compounds as FeSn and $FeSn_2$ (Fig. 7). As liquid tin has a higher density compared to

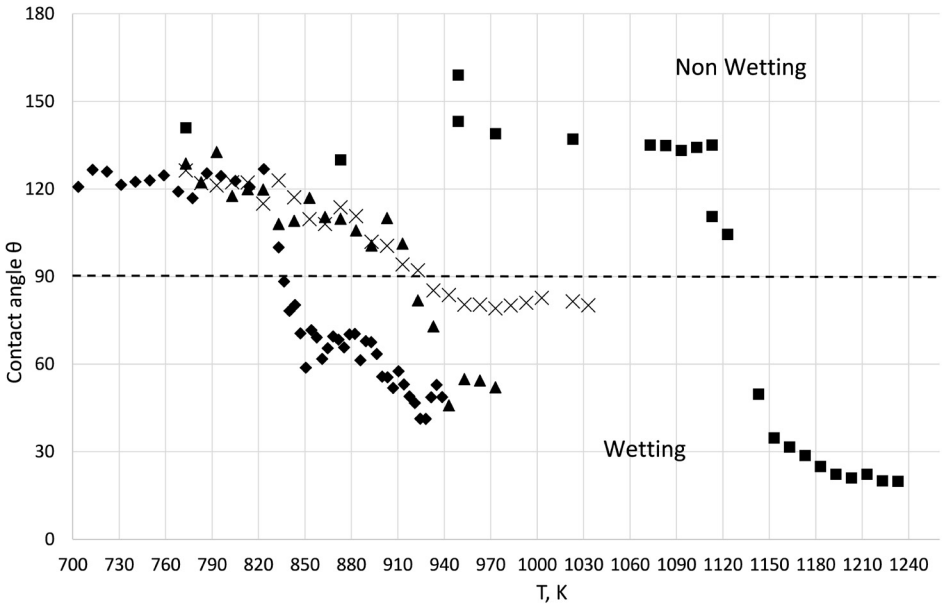

Fig. 5. Contact angles of liquid tin on the surface of different steels as function of temperature at residual pressure of 10^{-8} bar in vacuum. Different steels are denoted by different symbols: diamond: C45 steel, triangle: S103 steel, x: CK60 steel and squares: EN1.4034 steel

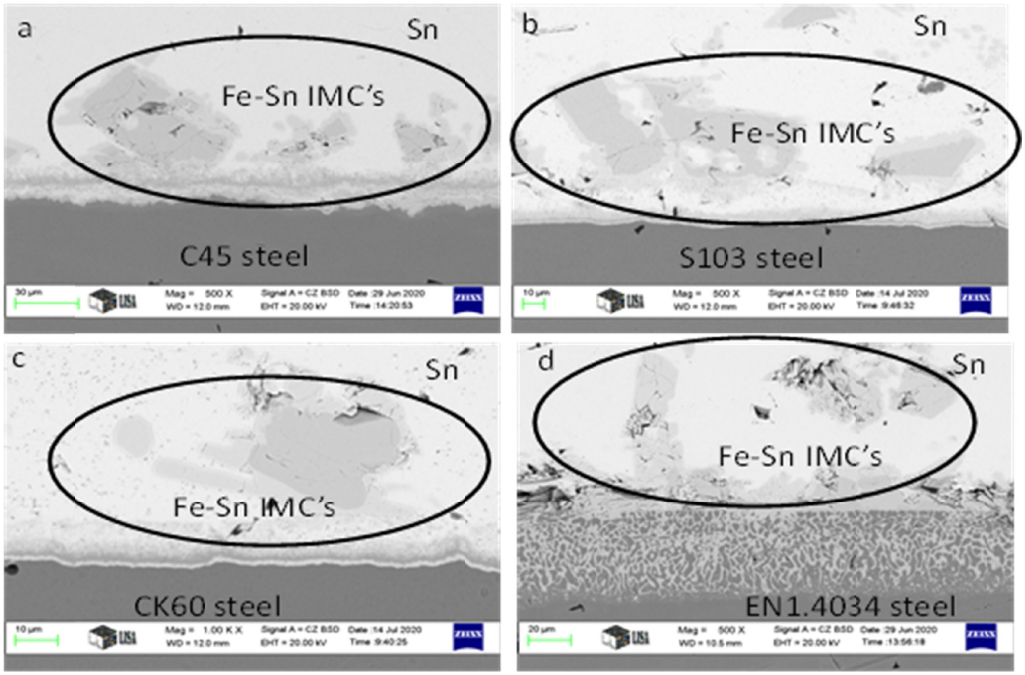

Fig. 6. SEM micrographs of cross-sectioned sessile drop couples showing intermetallic layers consisting of Fe/Sn compounds formed at the Sn/steel interface

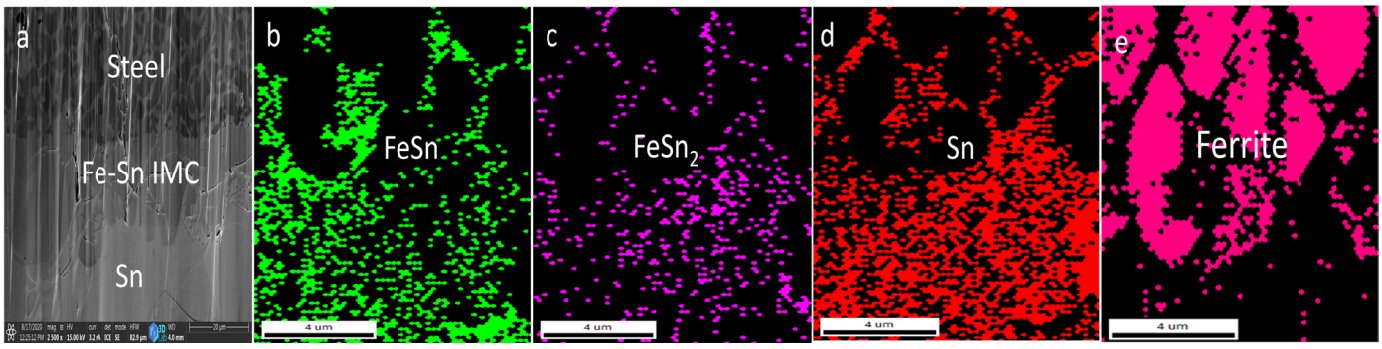

Fig. 7. EBSD analysis of the Sn/EN1.4034 steel interface (shown top down compared to macroscopic reality) with the identified phases. Fig. 7(a) shows the Sn/steel interface as observed under SEM. Figs. 7(b, c) show FeSn and $FeSn_2$ intermetallic compounds formed at the Sn/steel interface. Figs. 7(d, e) identify the presence tin and Fe elements in the image. Furthermore, the solidified Fe was identified as Ferrite in Fig. 7(e)

$FeSn_x$ intermetallics [51-52], the intermetallic particles will float up within liquid tin to the upper surface of the droplet. For the case of the longest holding time and the highest temperature, this even leads to the unexpected shape of the droplet (Fig. 4h).

It is important to note that the $FeSn_x$ intermetallic compounds are not fully metallic [53-54] and that is why the adhesion energy between them and liquid tin are considerably lower compared to usual metal/metal couples, such as at the Cu/Fe interface, forming no intermetallics [55-57]. This not fully-metallic behavior of the intermetallic compounds is further supported by the specific resistivity values of the Fe-Sn intermetallic compounds (FeSn and $FeSn_2$) as compared to the specific resistivity values of pure Fe and Sn in Fig. 8 [58-60]. The values of specific resistivity are one order of magnitude higher for the intermetallic compounds. This means that the intermetallic compounds are less conductive, i.e. less metallic than the pure metallic Fe and Sn. Let us mention that the formation of partly metallic intermetallics lead to the decrease of adhesion energy only relative to the metal/metal interfaces. However, if the initial interface is covalent with very low adhesion energy [61], then the formation of partly metallic IMCs actually leads to the increase of the adhesion energy, as is the case of the replacement of Al/C interface by Al/TiC interface [62].

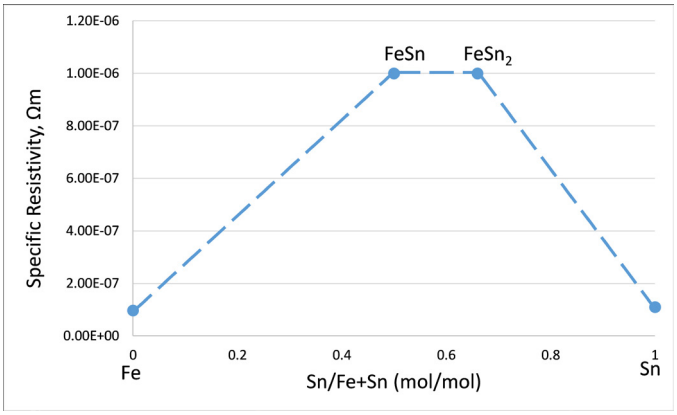

Fig. 8. Specific resistivity values of the intermetallic compounds identified at the steel/Sn interface compared to the special resistivity values of pure Fe and Sn at room temperature (T = 298 K) [58-60]

TABLE 2

Transition temperatures for liquid tin on various steels and the measured contact angles of liquid tin at temperatures above the transition temperature by 100 K (from Fig. 5)

Steel	Transition temperature (K) at 10^{-8} bar	Contact angle (°)
C45	833 ± 10	45 ± 10
S103	923 ± 10	50 ± 10
CK60	933 ± 10	80 ± 10
EN1.4034	1133 ± 10	20 ± 10

In some cases, the observed contact angle decreases upon heating due to evaporation of the droplet and decreasing its volume at constant base diameter. To make sure that in our experiments the non-wetting to wetting transition took place not due to the evaporation of the droplet, but rather because of the removal of the surface oxide layer, the base diameter and the height of the droplets were measured and plotted in Figs. 9-10. As follows from Figs. 9-10, the base diameter and height of the droplets as function of temperature are in qualitative agreement with Fig. 5 showing the temperature-dependence of contact angle. In other words, the change in the contact angle in Fig. 5 is accompanied by the appropriate changes in the base diameter and height of the droplets supposing no evaporation of the droplet. The absence of evaporation during our experiments is further confirmed by comparing the measured masses of the (steel + Sn) couples before and after high-temperature experiments (Table 3). This also follows from the low equilibrium vapor pressure of tin even at temperatures as high as 1230 K (Fig. 2).

TABLE 3

Measured mass of (steel + Sn) couples before and after the sessile drop tests

Steel	Before (g)		After (g)
	Steel	Sn	Steel +Sn
C45	2.21	0.04	2.25
S103	2.57	0.03	2.60
CK60	1.89	0.04	1.93
EN1.4034	2.14	0.02	2.16

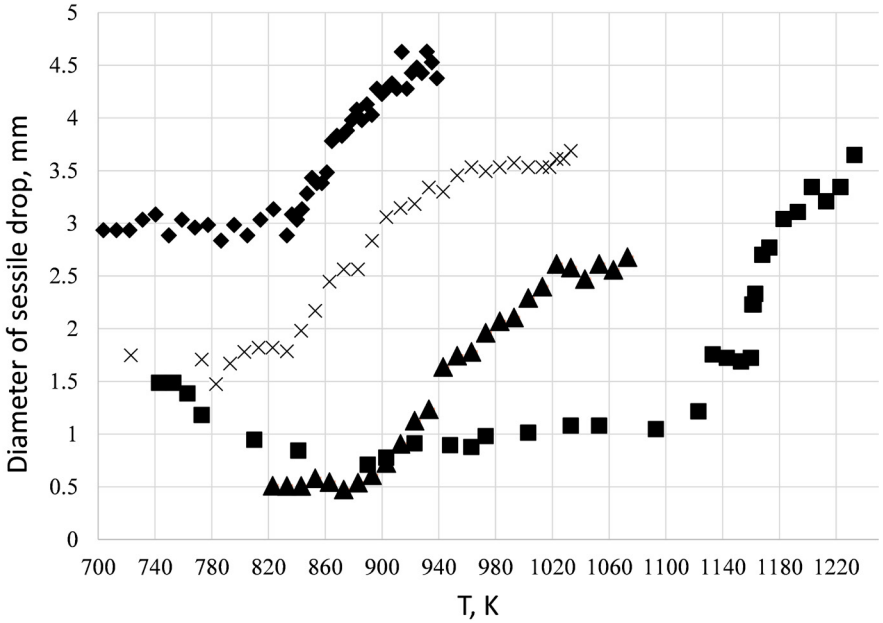

Fig. 9. Base diameter of the liquid tin sessile drops plotted against temperature for the 4 steel samples at 10^{-8} bar residual pressure in vacuum. Symbols: diamond: C45 steel, triangle: S103 steel, x: CK60 steel, square: EN1.4034 steel

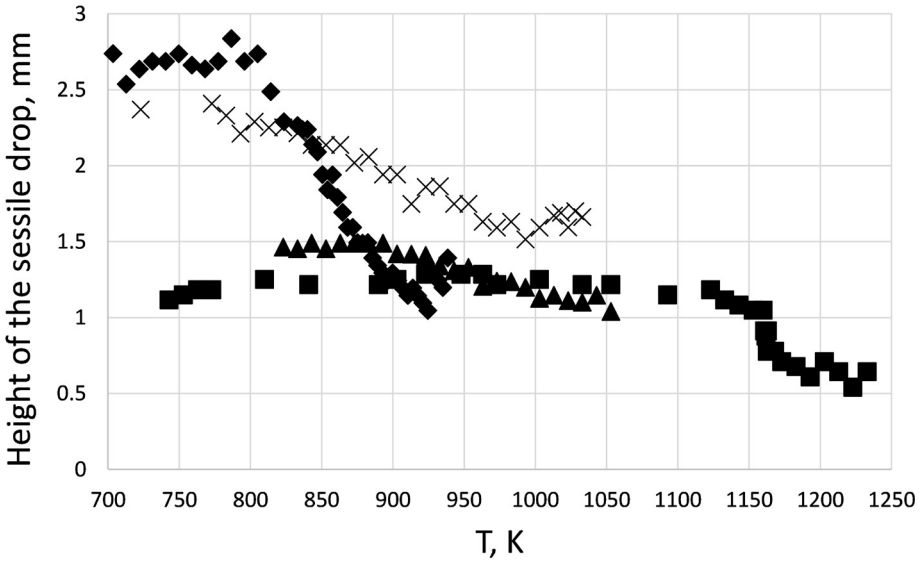

Fig. 10. Heights of the liquid tin sessile drops plotted against temperature for the 4 steel samples at 10^{-8} bar residual pressure in vacuum. Symbols: diamond: C45 steel, triangle: S103 steel, x: CK60 steel, square: EN1.4034 steel

5. Conclusions

- Non-wetting to wetting transition by liquid tin on the surface of four different steels was observed as function of temperature under vacuum at residual pressure of 10^{-8} bar. The transition temperature was measured and was found to depend on the compositions of steels.
- This observed transition is connected with the spontaneous removal of the oxide layers from the surface of steel samples due to the combined action of high temperature, low vacuum and the chemical reaction between the oxide layer and carbon content of the steels leading to the formation of volatile CO/CO_2 reaction products. This transition temperature was found in the range of 830-930 K for low alloyed C45, S103, CK60 steels, while the same was found around 1130 K for high chromium EN1.4034 steel (the latter value was in agreement with literature, while the other measured values are novel in the literature).
- Successful joining of steels without a flux is possible only above the transition temperatures found in this paper (under given residual pressure of around 10^{-8} bar). However, a flux removing the oxide layer should be applied for joining steels below the transition temperatures given here.
- Good wetting was achieved by liquid tin on all the steels after removal of the oxide layer from the surface of steels. Contact angles of liquid tin on steel surfaces were found

in the range of 45-80° for low alloyed C45, S103 and CK60 steels. The contact angle of liquid tin on the high Cr EN1.4034 steel was around 20°.

- The above mentioned relatively high contact angle values (if compared with metal/metal Cu/Fe system) are due to the formation of not fully metallic Fe/Sn intermetallics at the interface.

Acknowledgments

The research work presented are based on the results achieved within the GINOP2.3.2-15-2016-00027 "Sustainable operation of the workshop of excellence for the research and development of crystalline and amorphous nanostructured materials" project implemented in the framework of the Szechenyi 2020 Program. The realization of this project is supported by the European Union. The authors would like to thank Mrs. Aniko Markus and Mrs. Napsugar Nyari Bodnar for sample preparation.

REFERENCE

[1] T. Young, Philos. Trans. R. Soc. Lond. (95), 65-8 (1805).
[2] N. Eustathopoulos, M.G. Nicholas, B. Drevet, Wettability at high temperatures, Elsevier (1999).
[3] L. Yin, B.T. Murray, S. Su, Y. Sun, Y. Efraim, H. Taitelbaum, T.J. Singler, JOP: Condens. Matter. **21** (46), 464130 (2009).
[4] J. Bico, C. Tordeux, D. Quéré, Europhys. Lett. **55** (2), 214-22 (2001).
[5] N. Eustathopoulos, R. Voytovych, J. Mater. Sci. **51** (1), 425-43 (2016).
[6] M.L. Muolo, F. Valenza, N. Sobczak, A. Passerone, Adv. Sci. Technol. **64**, 98-10 (2010).
[7] R. Asthana, N. Sobczak, JOM-e **52** (1), 1-19 (2000).
[8] G.W. Liu, F. Valenza, M.L. Muolo, G.J. Qiao, A. Passerone, J. Mater. Sci. **44** (22), 5990-599 (2009).
[9] J. Janczak-Rusch, G. Kaptay, L.P.H. Jeurgens, J. Mater. Eng. Perform. **23**, 1608-13 (2014).
[10] G. Kaptay, Adv. Colloid. Interface Sci. **256**, 163-19 (2018).
[11] G. Kumar, K.N. Prabhu, Adv. Colloid Interf. Sci. **133** (2), 61-8 (2007).
[12] J. Yang, Q. Yuan, Y.P. Zhao, Int. J. Heat Mass Transf. **118**, 201-20 (2018).
[13] T J. Singler, S. Su, L. Yin, B.T. Murray, J. Mater. Sci. **47** (24), 8261-8274 (2012).
[14] A.M. Emelyanenko, L.B. Boinovich, Colloids Surf. A **189** (1-3), 197-20 (2001).
[15] N. Sobczak, M. Singh, R. Asthana, Curr. Opin. Solid State Mater. Sci. **9** (4-5), 241-25 (2005).
[16] N. Sobczak, R. Nowak, W. Radziwill, J. Budzioch, A. Glenz, Mater. Sci. Eng. **A 495** (1-2), 43-4 (2008).
[17] N. Eustathopoulos, N. Sobczak, A. Passerone, K. Nogi, J. Mater. Sci. **40** (9-10), 2271-228 (2005).
[18] Y.N. Chang, F.I. Wei, J. Mater. Sci. **24** (1), 14-2 (1989).
[19] R.Y. Chen, W.Y.D. Yeun, Oxidation Metals **59** (5-6), 433-46 (2003).
[20] A.M. Huntz, A. Reckmann, C. Haut, C. Sévérac, M. Herbst, F.C.T. Resende, A.C.S. Sabioni, Mater. Sci. Eng. A **447** (1-2), 266-27 (2007).
[21] A. Vesel, M. Mozetic, A. Drenik, N. Hauptman, M. Balat-Pichelin, Appl. Surf. Sci. **255** (5), 1759-176 (2008).
[22] O. Kozlova, R. Voytovych, M.F. Devismes, N. Eustathopoulos, Mater. Sci. Eng. A **495** (1-2), 96-101 (2008).
[23] O. Kozlova, R. Voytovych, P. Protsenko, N. Eustathopoulos, J. Mater. Sci. **45** (8), 2099-210 (2010).
[24] C.S. Doyle, C.K. Seal, B.J. James, Appl. Surf. Sci. **257** (23), 10005-10017 (2011).
[25] A.F. Rousseau, J.G. Partridge, Y.M. Gözükara, S. Gulizia, D.G. McCulloch, Vacuum **124**, 85-8 (2016).
[26] S. Pour-Ali, M. Weiser, N.T. Nguyen, A.R. Kiani-Rashid, A. Babakhani, S. Virtanen, Corros. Sci. **163**, 10828 (2020).
[27] Yu.V. Naidich, The wettability of solids by liquid metals. Progr. Surface Membrane Sci. **14**, 353-48 (1981).
[28] S.I. Popel, V.N. Kozhurkov, T.V. Zakharoya, Zaschschita Metallov. EnglishtTranslation **7**, 421-42 (1971).
[29] P. Protsenko, A. Terlain, V. Traskine, N. Eustathopoulos, Scr. Mater. **45** (12), 1439-144 (2001).
[30] Y. Takada, S. Shimada, J. Lee, M. Kurosaki, T. Tanaka, J. ISI, **93** (8), 532-53 (2007).
[31] Y. Kang, J. Han, H. Kim, J. Lee, Mater. Sci. **51** (4), 1713-172 (2016).
[32] J. Lee, T. Tanaka, M. Yamamoto, S. Hara, Mater. Trans. **45** (3), 625-62 (2004).
[33] T. Ishida, Mater. Sci. Technol. **4** (9), 830-83 (1988).
[34] S. Su, L. Yin, Y. Sun, B.T. Murray, T.J. Singler, Acta Mater. **57** (10), 3110-312 (2009).
[35] L. Yin, S.J. Meschter, T.J. Singler, Acta Mater. **52** (10), 2873-288 (2004).
[36] L. Yin, B T. Murray, T J. Singler, Acta Mater. **54** (13), 3561-357 (2006).
[37] P. Baumli, Mater. Sci. Eng. A (University of Miskolc) **40** (1), 42-4 (2015).
[38] S. Amore, E. Ricci, G. Borzone, R. Novakovic, Mater. Sci. Eng. A **495** (1-2), 108-112 (2008).
[39] Z. Weltsch, J. Hlinka, Mater. Eng. – Materiálové Inžinier (MEMI) **20** (1), 32-3 (2012).
[40] J. Hlinka, M. Berczeli, G. Buza, Z. Weltsch, Solder Surface Mount Technol. 69-7 (2017).
[41] J. Hlinka, Z. Fogarassy, A. Cziráki, Z. Weltsch, Appl. Surf. Sci. **501**, 14412 (2020).
[42] J. Hlinka, Z. Weltsch, MS&E **448** (1), 01202 (2018).
[43] J. Pstruś, P. Fima, T. Gancarz, J. Mater. Eng. Perf. **21** (5), 606-61 (2012).
[44] M.P. Kumar, G. Gergely, D. Koncz-Horvath, Z. Gacsi, Arch. Metall. Mater. **64**, 603-60 (2019).
[45] M.K. Pal, G. Gergely, D. Koncz-Horváth, Z. Gácsi, Powder Metall. Metal. Ceramics **58**, 529-53 (2020).
[46] M.K. Pal, G. Gergely, D. Koncz-Horváth, Z. Gácsi, Surf. Interf. 10057 (2020).
[47] S. Cheng, C.M. Huang, M. Pecht, Microelectron. Reliab. **75**, 77-9 (2017).

[48] N. Jiang, L. Zhang, Z.Q. Liu, L. Sun, W.M. Long, P. He, M. Zhao, Sci. Technol. Adv. Mater. **20** (1), 876-901 (2019).
[49] I. Barin, Thermochemical data of pure substances. Wiley-VCH, (1989).
[50] G. Kaptay, E. Báder, Trans. JWRI, 30 – S. I. 55-6 (2001)
[51] M.J. Assael, A.E. Kalyva, K.D. Antoniadis, R. Michael Banish, I. Egry, J. Wu, W.A. Wakeham, J. Phys. Chem. Ref. Data **39** (3), 03310 (2010).
[52] Y.S. Kwon, K.B. Gerasimov, S.S. Avramchuck, J. All. Comp. 3**59** (1-2), 79-8 (2003).
[53] R. Nesper, Angew. Chem. Int. Ed. **30** (7), 789-81 (1991).
[54] Stephan Hasse, Foundry lexicon, Foundry Technologies & Engineering GmbH, www.foundry-lexicon.com.
[55] T. Ishida, J. Mater. Sci. **21** (4), 1171-117 (1986).
[56] D. Varanasi, J.T. Szabo, P. Baumli, NanoWorld J. **5** (3), 36-4 (2019).
[57] Q. Sun, P. Jin, Y. Liu, J. Li, J. Wang, T. Ma, J. Feng, Mater. Des. 1**69**, 10766, (2019).
[58] B. Stenström, Phys, Script. **6** (4), 214-21 (1972).
[59] M. Armbrüster, W. Schnelle, R. Cardoso-Gil, Y. Grin, Chem. Eur. J. **16** (34), 10357-10365 (2010).
[60] S. Kasap, Handbook of electronic and photonic materials, Springer, (2006).
[61] E. Báder, L. Zoltai, M. Hördler, P. Arató, R.F. Singer, G. Kaptay, Trans. JWRI **30**, 137-14 (2001).
[62] P. Baumli, J. Sychev, I. Budai, J.T. Szabo, G. Kaptay, Compos. Part A **44**, 47-5 (2013).